



Growth of carbon nanofibers from methane on a hydroxyapatite-supported nickel catalyst

Ewa Miniach¹, Agata Śliwak¹, Adam Moyseowicz¹, and Grażyna Gryglewicz^{1,*}

¹Department of Polymer and Carbonaceous Materials, Faculty of Chemistry, Wrocław University of Technology, Gdańska 7/9, 50-344 Wrocław, Poland

Received: 25 October 2015

Accepted: 16 February 2016

Published online:

25 February 2016

© The Author(s) 2016. This article is published with open access at Springerlink.com

ABSTRACT

Carbon nanofibers (CNFs) were grown using catalytic chemical vapor deposition (CCVD) with methane as the carbon source and a hydroxyapatite-supported nickel catalyst (Ni/HAp). The catalyst, which contained approximately 14 wt% Ni, was prepared using the incipient wetness method with an aqueous nickel nitrate solution. Temperature-programmed reduction and X-ray diffraction were used to characterize the active phase of Ni/HAp. Three variables were evaluated to optimize the CNF growth process, including the temperature and the time of catalyst reduction as well as the reaction time, at 650 °C. Regardless of the applied CCVD process conditions, herringbone bamboo-like CNFs were grown during methane decomposition over Ni/HAp, which was confirmed using transmission electron microscopy. A high CNF yield of nearly $10 \text{ g}_{\text{CNF}} \text{ g}_{\text{cat}}^{-1}$ was achieved at 650 °C after a reaction time of 3 h when the catalyst was subjected to a reduction at the same temperature for 2 h under a hydrogen flow prior to synthesis. As the reduction temperature increased from 450 to 650 °C, both the yield and diameters of the CNFs increased. The beneficial effects of including hydrogen in the reaction mixture on the catalytic performance of Ni/HAp and the purity of the grown CNFs were demonstrated.

Introduction

Carbon nanofibers (CNFs), which include carbon nanotubes (CNTs), have been synthesized since the 1960s. However, the most significant discovery regarding CNTs was in 1991 when Iijima reported that highly graphitized carbon, which was formed from the arc discharge of graphite electrodes, contained several coaxial tubes and a hollow core [1].

Since this study was reported, the synthesis and application of CNFs/CNTs have attracted increasing interest due to their variety of extraordinary structures, which provide unique mechanical and electromagnetic properties, chemical inertness, high conductivity, surface properties, and ease of structure control [2]. Catalytic chemical vapor deposition (CCVD) using hydrocarbons is the most extensively used method to produce CNFs due to its high efficiency and selectivity at low costs. Many variables

Address correspondence to E-mail: grazyna.gryglewicz@pwr.edu.pl

affect CNF growth, such as the catalyst composition, reducibility of the catalyst, nature of the metal/support interaction, particle size of the active metal, synthesis temperature, carbon source, and composition of the reaction gas mixture [3–6]. The search for an efficient catalytic system that can provide good stability and dispersion of a catalytic active metal as well as high yield of well-defined carbon nanostructures remains the subject of much research [7, 8].

Methane decomposition over transition metals such as Ni, Fe or Co, is a promising approach for CNF synthesis due to the abundance and low cost of natural gas. Among the catalysts, Ni is characterized by exhibiting the highest catalytic activity in the production of CNFs [9, 10]. In most studies, Ni was deposited on widely used supports, such as Al₂O₃, SiO₂, TiO₂, MgO [11, 12], and zeolites [13] in addition to activated carbon [14, 15] and carbon nanofibers/nanotubes [16, 17]. Herein, we report the use of hydroxyapatite (HAp) as a support for a Ni catalyst to produce CNFs using methane decomposition. Only a few studies on the use of HAp as a catalyst support to produce CNF/HAp composites using a mixture of methane and nitrogen have been reported for potential applications in the dental and medical fields [18–20]. CNF-containing HAp-based composites are candidates for use in implants due to their enhanced mechanical properties [21–23]. The chemical inertness of HAp is an important property for a material that will be used as a catalyst support. HAp does not exhibit any catalytic activity during the high-temperature treatment [20] or create spinels that would lead to a reduction in the catalyst reducibility, which is often observed for alumina-supported nickel catalysts [24, 25]. Therefore, HAp appears to be a good support for Ni catalysts for the synthesis of CNF using CCVD.

In this study, selected variables of the CCVD process were studied to obtain CNFs with high yield and purity using a Ni/HAp catalyst and methane as the carbon source. We focused on the catalyst reduction conditions in the CCVD process because they are rarely reported in the literature. Our results demonstrate that the optimization of the temperature and time of catalyst reduction is crucial for high-yield CNF synthesis. For optimal reduction conditions, the kinetics of CNF growth were studied to evaluate the susceptibility of Ni/HAp to deactivation.

Experimental

Catalyst preparation

Hydroxyapatite (HAp) with a purity grade of 97 % (Sigma-Aldrich, particle size <200 nm) was used as the support. The HAp-supported Ni catalyst was prepared using the incipient wetness method with an aqueous solution of Ni(NO₃)₆H₂O (ACROS Organics, 99 %). The amount of Ni precursor was adjusted to achieve a Ni weight loading of 14 wt% in the catalyst. The sample was further dried at 110 °C for 2 h and subsequently calcined in a nitrogen atmosphere at 350 °C for 4 h. The Ni content in the catalyst was determined to be 13.4 wt% using atomic absorption spectroscopy (AAS). The prepared catalyst is referred to as Ni/HAp.

Synthesis of CNFs

CNFs were synthesized using CCVD with methane as the carbon precursor. First, 200 mg of the Ni/HAp catalyst was loaded in a quartz boat and placed in a quartz tube in the central heat zone of a conventional horizontal furnace. Prior to CNF growth, the catalyst was reduced under hydrogen flowing at a rate of 150 ml min⁻¹ at various temperatures (450–650 °C) and times (10–120 min). After the reduction, a mixture of CH₄ and H₂ (1:1, v/v, 150 ml min⁻¹) was passed through the quartz tube at 650 °C. The reaction time was varied from 3 to 180 min. The resulting CNFs were subsequently cooled to ambient temperature in a nitrogen atmosphere. Both the catalyst reduction and the CNF synthesis were performed at atmospheric pressure. The purity grades of CH₄, H₂, and N₂ were 99.995, 99.999, and 99.999 %, respectively.

The yield (*Y*) of CNFs was calculated based on the catalyst weight increase during the reaction using the following equation:

$$Y = \frac{m_t - m_{\text{cat}}}{m_{\text{cat}}}, \quad (1)$$

where *Y* is the yield of CNF expressed in g_{CNF} per g_{cat} [g_{CNF} g_{cat}⁻¹], *m_t* is the total weight of the catalyst and the deposited carbon at the end of the reaction, and *m_{cat}* is the initial mass of the catalyst. Additionally, the yield (*Y_{Ni}*) was expressed per gram of metal (g_{CNF} g_{Ni}⁻¹) according to the following equation:

$$Y_{\text{Ni}} = \frac{m_t - m_{\text{cat}}}{0.134 \cdot m_{\text{cat}}} \quad (2)$$

The difference in the CNF yield for two separate runs, which were performed using the same experimental conditions, was not higher than 7 % of the average yield. The as-received CNFs were treated with 5 % HCl for 2 h at room temperature in a sonication bath to remove the nickel and hydroxyapatite. Subsequently, the samples were washed with distilled water, filtered, and dried at 110 °C for 2 h.

Catalyst characterization

The nickel content in the Ni/HAp catalyst was determined by AAS using a SOLAAR S4 spectrometer. Temperature-programmed reduction (TPR) was performed on a ChemBET 3000 analyzer (Quantachrome) using a reducing mixture of H₂ (5 % v/v)–Ar (100 ml min⁻¹). The catalyst sample was heated at a rate of 20 °C min⁻¹ from ambient temperature to 980 °C. The hydrogen consumption was determined using CuO as a standard for the TPR analysis. X-ray diffraction (XRD) analysis was performed on an Ultima IV Rigaku diffractometer using CuK α radiation ($\lambda = 1.54056 \text{ \AA}$). The average sizes of the NiO and Ni crystallites were calculated using Scherrer's equation.

CNF characterization

The morphologies of the as-grown and purified CNFs, HAp, and as-prepared Ni/HAp catalyst were studied using scanning electron microscopy (SEM) on an EVO LS15 Zeiss microscope. The arrangement of graphene layers in the CNFs was determined by transmission electron microscopy (TEM) using a FEI Tecnai G² 20 X-TWIN microscope, which was operated at an acceleration voltage of 200 kV. The sample was prepared by ultrasonic dispersion in ethanol, and a few drops of the suspension were placed onto a copper microgrid covered with a perforated carbon film. The average CNF diameter was determined based on the measurement of 50 nanofibers for each sample. Thermogravimetric analysis (TGA) was performed on the purified CNFs using a TGA/DSC1 Mettler Toledo (thermobalance).

Results and discussion

Catalyst characterization

Figure 1 shows the X-ray diffraction patterns of the as-prepared (a) and reduced Ni/HAp (b) catalysts. For the as-prepared Ni/HAp catalyst, we observed diffraction peaks arising from different planes of the NiO phase (i.e., $2\theta = 37.2^\circ$ (111), 43.2° (200), 62.9° (220), 75.5° (311), and 79.5° (222)) (Fig. 1a) [ICSD No:01-1239]. The diffraction peaks at $2\theta = 25.9^\circ$ (002), 29.0° (210), 31.8° (211), 32.2° (112), 32.9° (300), 34.0° (202), 39.8° (310), 46.7° (222), 49.5° (213), 50.5° (321), and 53.1° (004) were due to the crystalline Ca₅(PO₄)₃(OH) phase. The average size of the NiO crystallites, which was determined using XRD, was 22 nm for the fresh Ni/HAp catalyst. After catalyst reduction at 650 °C for 2 h, the XRD pattern (Fig. 1b) showed diffraction peaks arising from metallic Ni (i.e., $2\theta = 44.4^\circ$ (111), 51.8° (200), and 76.4° (220)) [ICSD No:04-0850]. The Ni crystallite size was bigger than that of NiO (34 vs. 22 nm), suggesting sintering and aggregation of the nickel phase during the heat treatment in a hydrogen atmosphere. The strong influence of the metal particle size on the CNF yield has been previously reported [7, 26, 27]. Excessively small metal particles will not form CNFs because the quantity of metal is not sufficient to enable CNF formation according to the proposed mechanism of CNF growth during CCVD. In contrast, excessively large metal particles are inactive because the carbon diffusion through these particles is hindered [28]. Chen et al. [7] reported the relationship between the NiO particle size of a hydroxycalcite-supported catalyst and the yield of CNFs produced from methane decomposition. The most suitable NiO particle sizes, which constitute the catalytic centers for CNF growth after the hydrogen treatment, were determined to be approximately 34 nm. Moreover, based on XRD analysis, the average NiO crystal size of the as-prepared catalyst was comparable to the Ni crystal size of the reduced catalyst, which was determined by chemisorption [7]. Therefore, the synthesized Ni/HAp catalyst with an average Ni crystallite size of 34 nm appears to be a promising catalytic system for CNF growth. Some studies [26, 27] have reported that Ni particles with sizes of 10–60 nm are characteristic of highly active catalysts for the production of CNFs via methane decomposition.

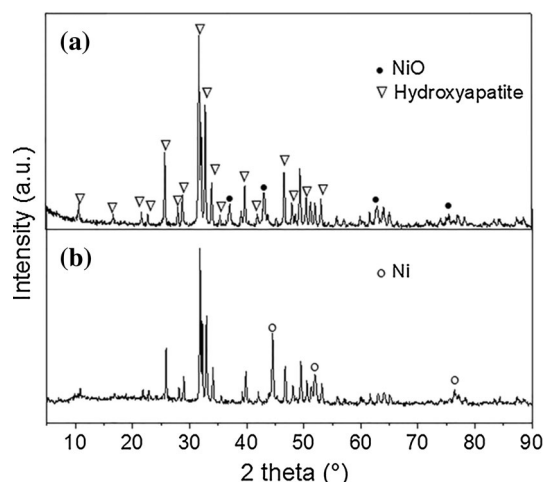


Figure 1 XRD pattern of the fresh Ni/HAp catalyst (a) and reduced Ni/HAp catalyst (b).

The morphology of the as-prepared Ni/HAp catalyst was very similar to that of the support (Fig. S1). The HAp powder consists of agglomerated spherical nanoparticles, and their sizes are preserved in the Ni/HAp catalyst. SEM-EDX investigation of the reduced Ni/HAp catalyst revealed that nickel was homogeneously distributed on the surface of the support particles (Fig. S2).

The reducibility of the Ni/HAp catalyst, which was characterized by the TPR profile, is shown in Fig. 2. Only one wide peak with a maximum at 470 °C was observed due to the reduction of NiO to metallic Ni. A small shoulder on the curve at approximately 380 °C may correspond to the reduction of very fine NiO particles. The reduction of NiO began at 200 °C and ended at 670 °C. The hydrogen consumption determined by TPR was 2.08 mmol g⁻¹.

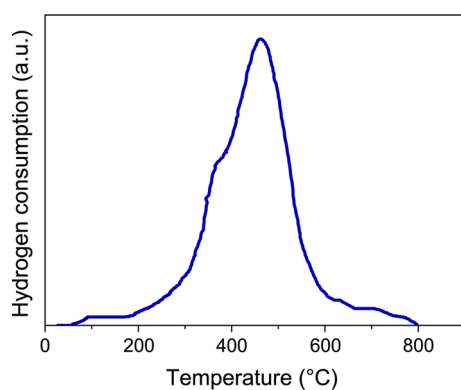


Figure 2 TPR profile of the Ni/HAp catalyst.

Effect of the reduction temperature

Based on the TPR results, a temperature range of 450 to 650 °C was selected to determine the effect of the Ni/HAp reduction temperature on the yield, morphology, and structure of the grown CNFs. The CNFs were synthesized at 650 °C using methane diluted with hydrogen in a ratio of 1:1 (v/v). The reduction time was 2 h. The CNF yields, which depend on the reduction temperature of the Ni/HAp catalyst, are listed in Table 1. As the reduction temperature increased from 450 to 650 °C, the CNF yield increased from 3.9 to 5.9 g_{CNF} g_{cat}⁻¹, which may be due to the increasing number of Ni active sites on the catalyst surface. The latter result is supported by the TPR profile of Ni/HAp (Fig. 2), which indicates that approximately half of the NiO was reduced to the metallic form at 450 °C. Pronounced CNF growth was observed up to 600 °C, but further CNF growth was only slightly higher at 650 °C. As expected, this growth was followed by an increase in the amount of Ni, which contributed to the CNF growth and yielded 42.5 g_{CNF} g_{Ni}⁻¹ at 650 °C compared to 27.6 g_{CNF} g_{Ni}⁻¹ at 450 °C. An enhancement in CNF growth from methane over a Ni–Cu–MgO catalyst with an increase in the reduction temperature from 600 to 1000 °C has also been reported by Wang et al. [29].

Figure 3 shows the TEM images of the as-grown CNFs, which were synthesized over the Ni/HAp catalyst and reduced at different temperatures. Regardless of the reduction temperature, the graphene layers were stacked at an angle to the fiber axis, which indicates the presence of their herringbone structural type. The herringbone bamboo-like CNFs were primarily grown on the surface of the Ni/HAp catalyst. CNFs with a herringbone-type graphene layer arrangement exhibit open edges on their outer surface, which result in high chemical activity and may be beneficial in medical and other applications. The presence of Ni particles at the ends of the

Table 1 Effect of the Ni/HAp reduction temperature on CNF growth

Temperature (°C)	Reaction yield	
	(g _{CNF} g _{cat} ⁻¹)	(g _{CNF} g _{Ni} ⁻¹)
450	3.9	27.6
550	4.2	30.3
600	5.8	41.6
650	5.9	42.5

nanofibers suggests a tip-growth mechanism due to weak catalyst-support interactions [8]. The herringbone type of CNFs is a typical structure that forms during CCVD when using methane over a Ni catalyst [30]. The diameters of the grown CNFs were determined by TEM. As shown in Fig. 4, the CNF diameters increased as the reduction temperature increased. At 550 °C, CNFs with a diameter of 25–45 nm were grown with a predominant contribution of narrower nanofibers. At 600 °C, a wide distribution of CNF diameters in the range of 25–55 nm was observed. CNFs with a diameter of 36–55 nm were obtained when the Ni/HAp catalyst was reduced at 650 °C. The shift in the CNF diameter to larger values as the reduction temperature increases was due to an increase in the Ni crystallite size. CNFs with larger diameters were also grown by increasing the reaction temperature [16, 31].

An increase in the reduction temperature can lead to the migration of nickel particles on the support surface and formation of larger agglomerates, which results in larger CNF diameters. However, the catalyst, operating conditions, and reactant gas composition affect the CNF diameters [32]. In our study, the most suitable temperature for Ni/HAp reduction was determined to be 650 °C, which results in maximum reduction of the NiO phase.

Effect of the reduction time

In general, a higher amount of NiO reduced to a metallic form corresponds to a higher CNF yield. The extent of catalyst reduction depends on both the temperature and reduction time. The effect of the

reduction time on CNF growth was investigated at 650 °C, where the maximum conversion of NiO to Ni was observed. After catalyst reduction, the CNFs were synthesized at the same temperature for 1 h using a mixture of methane and hydrogen at a ratio of 1:1 (v/v). Figure 5 shows the effect of the reduction time on the CNF growth over Ni/HAp. An increase in the catalyst reduction times led to a higher CNF yield, which is due to the increased amounts of reduced metallic nickel. A maximum CNF weight gain ($5.9 \text{ g}_{\text{CNF}} \text{ g}_{\text{cat}}^{-1}$) was obtained at 2 h of reduction. A sharp increase in CNF growth was observed for up to 30 min of reduction, and then, the growth rate subsequently decreased. The plateau in the plot of the yield as a function of the reduction time indicates that 2 h is an optimal time for activation of all of the catalytic Ni centers on the HAp surface. Longer reduction times most likely promote the formation of large agglomerates of Ni, which are unable to catalyze the decomposition of methane.

Figure 6 shows the SEM images of the obtained CNFs at different Ni/HAp reduction times. After 10 min of reduction, the CNFs were heterogeneously dispersed on the catalyst surface and characterized by a broad size distribution, which ranged from short to several micrometers in length (Fig. 6a). An increase in the reduction time to 60 min produced a strong entangled network of nanofibers that were more than a dozen micrometers in length (Fig. 6b). A dense network of entangled nanofibers was observed when Ni/HAp was reduced at 650 °C for 2 h. The obtained results indicate that a reduction time of 2 h is optimal for CNF production over the Ni/HAp catalyst.

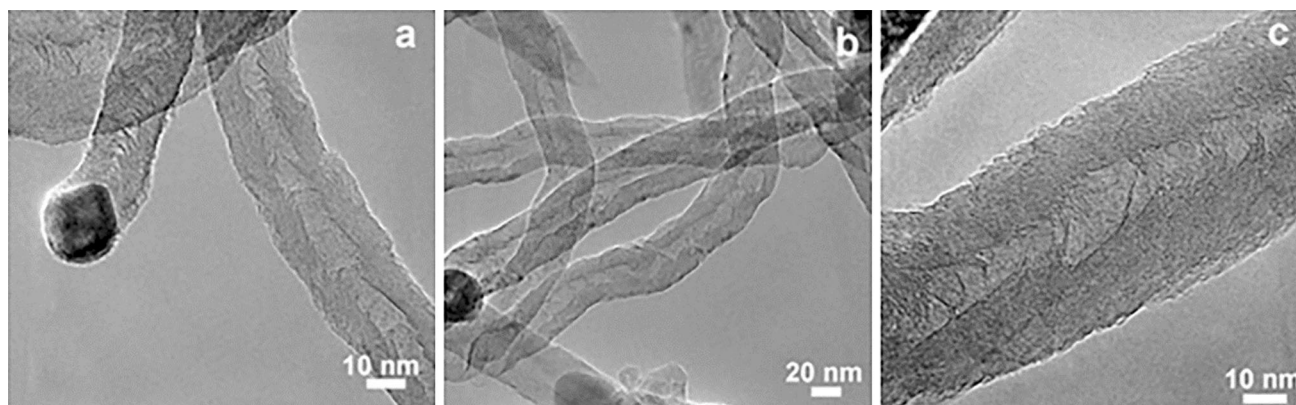


Figure 3 TEM images of CNFs synthesized with a catalyst reduction at 550 °C (a), 600 °C (b), and 650 °C (c).

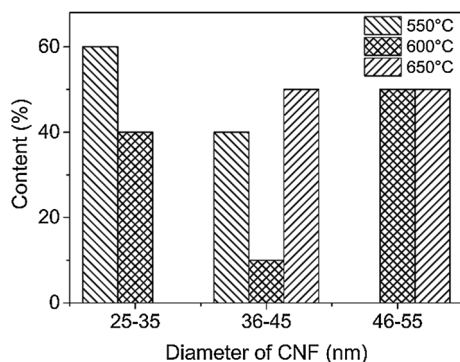


Figure 4 Diameter distribution of CNFs as a function of the reduction temperature of Ni/HAp.

Kinetics of CNF growth

The temperature of CCVD is crucial to the growth of CNFs [13, 17]. For a given catalyst, the temperature must be higher than the decomposition temperature of the carbon precursor on the catalyst surface. An increase in the synthesis temperature results in an enhanced CNF yield but only to a certain extent. Excessive temperatures promote the uncontrolled deposition of carbon as well as the migration of metallic catalyst nanoparticles across the surface, resulting in the formation of large nanoparticles that do not promote CNF growth. An increase in reaction temperature up to 600–650 °C increases methane conversion to filamentous carbon and hydrogen over Ni catalysts [33], which is consistent with results for Ni catalysts that exhibit the highest activity toward methane decomposition at 650 °C [34]. In our study, the kinetic study of the CNF growth over Ni/HAp was performed at 650 °C using a mixture of CH₄ and H₂. Prior to CNF growth, the Ni/HAp catalyst was reduced with hydrogen under the previously determined optimal conditions (i.e., at 650 °C for 2 h). Figure 7 shows the CNF yield as a function of the synthesis time.

An increase in the CNF productivity from 0.15 to 9.92 g_{CNF} g_{cat}⁻¹ was observed when the reaction time was increased from 3 to 180 min. During the first few minutes of the process, only a small portion of Ni contributed to the CNF growth (1.12 g_{CNF} g_{Ni}⁻¹). After 180 min, a large amount of Ni was involved in CNF growth (74.03 g_{CNF} g_{Ni}⁻¹). The highest rate of CNF growth was observed during the first hour of synthesis. At longer reaction times, the growth of the CNFs slightly decreased. The high yield of CNFs

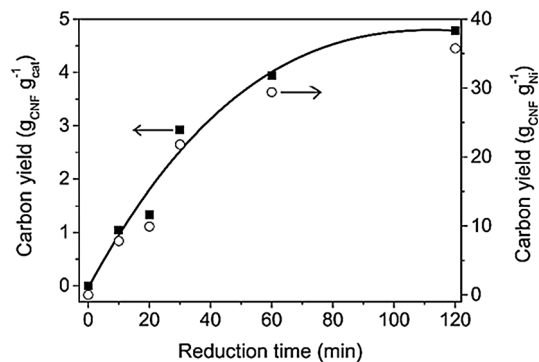


Figure 5 Relationship between the CNF yield and the reduction time of Ni/HAp at 650 °C.

after 3 h of synthesis (nearly 10 g_{CNF} g_{cat}⁻¹) was due to the large amount of the nickel active phase, which results from the hydrogen in the reaction gas mixture preventing deposition of amorphous carbon on the catalyst surface. The presence of hydrogen in the reaction mixture plays a crucial role in the formation of CNFs due to the decomposition of hydrocarbons [31, 35]. Hydrogen can either accelerate or suppress the formation of carbon [36], which affects the yield and morphology of the resulting CNFs as well as catalyst deactivation. This effect can be interpreted in multiple ways. Hydrogen, which is present in the feed stream along with methane, may be responsible for the decomposition of nickel carbides to form catalytically active metal particles [37] or remove the graphite overlayer that encapsulates the catalyst active surface [38]. In our study, hydrogen undoubtedly facilitates CNF growth by maintaining the catalytic activity of Ni, which leads to a high CNF yield. A continuous weight gain of CNFs with synthesis time may be related to hydrogen activation of new catalytic centers that were not activated during the catalyst reduction step. The two processes can occur simultaneously (i.e., the reduction of NiO nanoparticles to create new active sites for CNF growth and the decomposition of methane on previously activated Ni centers, which both lead to an increase in the length of nanofibers). This result is supported by SEM investigations of the CNFs obtained using different synthesis times (Fig. 8).

After a reaction time of 3 min, the catalyst surface was not entirely coated with CNFs, which were several micrometers in length (Fig. 8a). Much longer and entangled CNFs appeared after a longer synthesis time (Fig. 8b). The increasing number of nanofibers

Figure 6 SEM images of the CNFs obtained after 10 min (a) and 60 min (b) of Ni/HAp reduction.

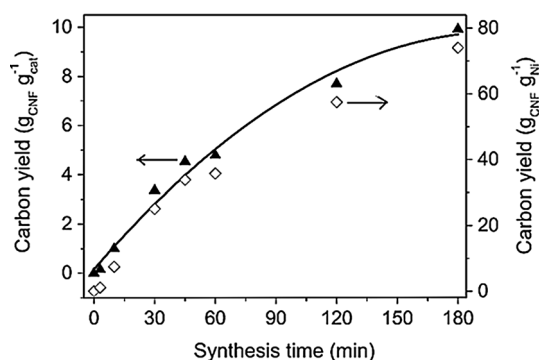
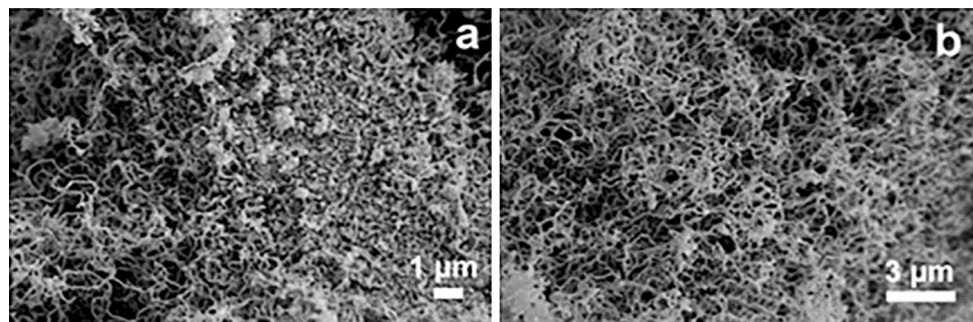


Figure 7 CNF growth as a function of the synthesis time over the Ni/HAp catalyst at 650 °C.

on the support surface suggests the creation of new active sites during CCVD, which is supported by the higher CNF yield expressed as $g_{\text{CNF}} g_{\text{Ni}}^{-1}$. After a reaction time of 180 min, the entire surface was coated with a dense layer of strongly entangled nanofibers that were 10 μm in length (Fig. 8c), providing a yield of approximately 10 $g_{\text{CNF}} g_{\text{cat}}^{-1}$. It is important to note that by adjusting the reaction time, CNF/HAp composites with adjustable CNFs contents and lengths can be tailored for specific requirements.

The beneficial effect of hydrogen on the CNF growth over Ni/HAp using methane as a carbon

precursor can also be demonstrated by comparing the obtained CNF yields with those reported by Ashok et al. [20]. The Ni/HAp catalyst with 15 wt% of Ni after 4 h of synthesis at 650 °C in a methane stream (without hydrogen) produced 0.76 $g_{\text{CNF}} g_{\text{cat}}^{-1}$ of CNFs. In our study, a mixture of methane and hydrogen resulted in a CNF yield that was several times greater to as high as 9.92 $g_{\text{CNF}} g_{\text{cat}}^{-1}$. Few studies of Ni catalysts based on different supports with high performance in hydrocarbon decomposition to produce CNFs have been reported (e.g., Ni/Al₂O₃ with 90 wt% of metal loading) [39]. This catalyst enabled a CNF yield of 20 $g_{\text{CNF}} g_{\text{cat}}^{-1}$ after 2 h of reaction. However, the difficulties associated with the thermal instability of Al₂O₃ and its low mechanical strength have been reported by Boukha et al. [25]. Moreover, alumina can create spinels with nickel, which prevents the formation of nickel growth centers [25]. Based on these negative features, alumina can be replaced by other promising Ni catalyst supports, such as the studied hydroxyapatite, which has excellent mechanical properties and does not react with nickel.

It is interesting to note that although notably high yields of CNFs were obtained, amorphous carbon was not formed during the CCVD process, which

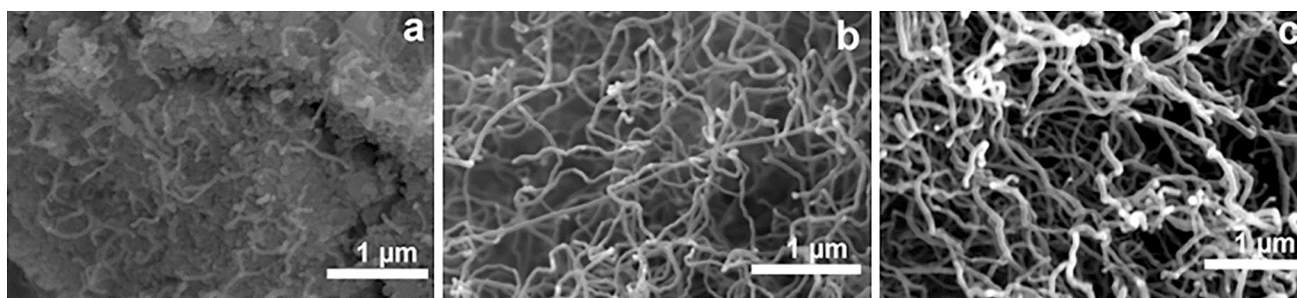


Figure 8 SEM images of CNFs synthesized at 650 °C for 3 min (a), 60 min (b), and 180 min (c).

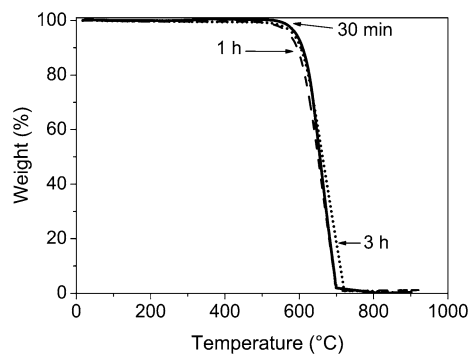


Figure 9 TGA curves of CNFs synthesized with different reaction times.

was confirmed by SEM analysis. This result suggests that the presence of hydrogen in the reaction mixture efficiently prevents the deposition of undesirable carbon. The TGA analysis revealed a similar oxidation behavior of the resulting CNFs regardless of the synthesis time (Fig. 9).

The weight loss, which may be due to the non-crystalline structure of carbonaceous materials, such as amorphous carbon, occurred between 300 and 400 °C. In this temperature range, no oxidation was observed even for the CNFs synthesized for 3 h. This result demonstrates that a highly ordered graphitic structure without amorphous carbon is characteristic of CNFs that are synthesized over Ni/HAP using a CH₄ and H₂ mixture.

Conclusions

This study demonstrates that the use of hydroxyapatite as a support for a nickel catalyst results in the production of herringbone bamboo-like CNFs in a high yield with no amorphous carbon by CCVD using a mixture of methane and hydrogen as the reactant gas. At a reaction temperature of 650 °C, the growth of CNFs and their diameter distribution strongly depended on the catalyst reduction temperature. An increase in the reduction temperature of Ni/HAP from 450 to 650 °C increased the CNF growth due to the larger amount of reduced metallic nickel. Moreover, reduction at higher temperatures produced CNFs with larger diameters due to agglomeration of nickel particles during the high-temperature treatment. This result suggests that the diameter distribution of the grown CNFs can be tailored by adjusting the reduction temperature of the catalyst. A notably

high CNF yield up to approximately $10 \text{ g}_{\text{CNF}} \text{ g}_{\text{cat}}^{-1}$ was obtained at 650 °C with a reaction time of 3 h when Ni/HAP was reduced at 650 °C for 2 h. At this temperature, all of the reducible NiO in the Ni/HAP catalyst was converted to the metallic form, which was confirmed by TPR. Due to the inertness of hydroxyapatite and the presence of hydrogen in the reaction mixture, the Ni/HAP catalyst was resistant to deactivation and maintained its catalytic activity during CNF growth over long CCVD processing times. Due to the graphitic edges that were exposed on the outer surface of the herringbone CNFs, this structure has a high potential for modification, which may create new applications for CNF/HAP composites.

Acknowledgements

This work was financed by a statutory activity subsidy from the Polish Ministry of Science and Higher Education for the Faculty of Chemistry of Wrocław University of Technology. The project was supported by Wrocław Centre of Biotechnology, under The Leading National Research Centre (KNOW) programme for years 2014–2018.

Compliance with ethical standards

Conflict of interest The authors declare that they have no conflict of interest.

Open Access This article is distributed under the terms of the Creative Commons Attribution 4.0 International License (<http://creativecommons.org/licenses/by/4.0/>), which permits unrestricted use, distribution, and reproduction in any medium, provided you give appropriate credit to the original author(s) and the source, provide a link to the Creative Commons license, and indicate if changes were made.

Electronic supplementary material: The online version of this article (doi:10.1007/s10853-016-9839-1) contains supplementary material, which is available to authorized users.

References

- [1] Iijima S (1991) Helical microtubules of graphitic carbon. *Nature* 354:56–58

- [2] Feng L, Xie N, Zhong J (2014) Carbon nanofibers and their composites: a review of synthesizing, properties and applications. *Materials* 7:3919–3945
- [3] Zhou JH, Sui ZJ, Li P, Chen D, Dai YC, Yuan WK (2006) Structural characterization of carbon nanofibers formed from different carbon-containing gases. *Carbon* 44:3255–3266
- [4] Tessonier JP, Rosenthal D, Hansen TW, Hess Ch, Schuster ME, Blume R, Girsadies F, Pfander N, Timpe O, Su DS, Schlogl R (2009) Analysis of the structure and chemical properties of some commercial carbon nanostructures. *Carbon* 47:1779–1798
- [5] Moysowicz A, Śliwak A, Gryglewicz G (2016) Influence of structural and textural parameters of carbon nanofibers on their capacitive behavior. *J Mater Sci* 51:3431–3439. doi:10.1007/s10853-015-9660-2
- [6] Yu L, Qin Y, Sui L, Zhang Q, Cui Z (2008) Two opposite growth modes of carbon nanofibers prepared by catalytic decomposition of acetylene at low temperature. *J Mater Sci* 43:883–886. doi:10.1007/s10853-007-2191-8
- [7] Chen D, Christensen KO, Ochoa-Fernandez E, Yu Z, Totdal B, Latorre N, Monzon A, Holmen A (2005) Synthesis of carbon nanofibers: effects of Ni crystal size during methane decomposition. *J Catal* 229:82–96
- [8] Vander Wal RL, Ticich TM, Curtis VE (2001) Substrate-support interactions in metal catalyzed carbon nanofiber growth. *Carbon* 39:2277–2289
- [9] Yamada Y, Hosono Y, Murakoshi N, Higashi N, Ichi-oka H, Miyake T et al (2006) Carbon nanofiber formation on iron group metal loaded on SiO₂. *Diam Relat Mater* 15(4–8):1080–1084
- [10] Romero A, Garrido A, Nieto-Marquez A, Sanchez P, de Lucas A, Valverde JL (2008) Synthesis and structural characteristics of highly graphitized carbon nanofibers produced from the catalytic decomposition of ethylene: influence of the active metal (Co, Ni, Fe) and the zeolite type support. *Microporous Mesoporous Mater* 110(2–3):318–329
- [11] Takenaka S, Shigeta Y, Tanabe E, Otsuka K (2003) Methane decomposition into hydrogen and carbon nanofibers over supported Pd-Ni catalysts. *J Catal* 220:468–477
- [12] Li Y, Li D, Wang G (2011) Methane decomposition to CO_x-free hydrogen and nano-carbon material on group 8–10 base metal catalysts: a review. *Catal Today* 162:1–48
- [13] De Lucas A, Garrido A, Sanchez P, Romero A, Valverde JL (2005) Growth of carbon nanofibers from Ni/Y zeolite based catalysts: effects of Ni introduction method, reaction temperature, and reaction gas composition. *Ind Eng Chem Res* 44:8225–8236
- [14] Rinaldi A, Abdullah N, Ali M, Furche A, Bee Abd Hamid S, Sheng Su S, Schlogl R (2009) Controlling the yield and structure of carbon nanofibers grown on a nickel/activated carbon catalyst. *Carbon* 47:3023–3033
- [15] Gryglewicz G, Śliwak A, Beguin F (2013) Carbon nanofibers grafted on activated carbon as an electrode in high-power supercapacitors. *ChemSusChem* 6:1516–1522
- [16] Romero A, Garrido A, Nieto-Marquez A, Raquel de la Oa A, de Lucas A, Valverde JL (2007) The influence of operating conditions on the growth of carbon nanofibers on carbon nanofiber-supported nickel catalyst. *Appl Catal A* 319:246–258
- [17] Zhao Y, Li Ch, Yao K, Liang J (2007) Preparation of carbon nanofibers over carbon nanotube-nickel catalyst in propylene decomposition. *J Mater Sci* 42:4240–4244. doi:10.1007/s10853-006-0676-5
- [18] Li H, Zhao N, Liu Y, Liang C, Shi C, Du X, Li J (2008) Fabrication and properties of carbon nanotubes reinforced Fe/hydroxyapatite composites by in situ chemical vapor deposition. *Compos A* 39(7):1128–1132
- [19] Li H, Wang L, Liang C, Wang Z, Zhao W (2010) Dispersion of carbon nanotubes in hydroxyapatite powder by in situ chemical vapor deposition. *Mater Sci Eng B* 166(1):19–23
- [20] Ashok J, Naveen Kumar S, Subrahmanyam M, Venugopal A (2008) Pure H₂ production by decomposition of methane over Ni supported on hydroxyapatite catalyst. *Catal Lett* 121:283–290
- [21] Kaya C (2008) Electrophoretic deposition of carbon nanotube-reinforced hydroxyapatite bioactive layers on Ti-6Al-4 V alloys for biomedical applications. *Ceram Int* 34:1843–1847
- [22] Mukherjee S, Kundu B, Sen S, Chanda A (2014) Improved properties of hydroxyapatite–carbon nanotube biocomposite: mechanical, in vitro bioactivity and biological studies. *Ceram Int* 40:5635–5643
- [23] Prodana M, Duta M, Ionita D, Bojin D, Stan MS, Dinischiotu A, Demetrescu I (2015) A new complex ceramic coating with carbon nanotubes, hydroxyapatite and TiO₂ nanotubes on Ti surface for biomedical applications. *Ceram Int* 41:6318–6325
- [24] Piao L, Li Y, Chen J, Chang L, Lin JYS (2002) Methane decomposition to carbon nanotubes and hydrogen on an alumina supported nickel aerogel catalyst. *Catal Today* 74(1–2):145–155
- [25] Boukha Z, Jimenez-Gonzalez C, de Rivas B, Gonzalez-Velasco JR, Gutierrez-Ortiz JI, Lopez-Fonseca R (2014) Synthesis, characterization and performance evaluation of spinel-derived Al₂O₃ catalysts for various methane reforming reactions. *Appl Catal B* 158–159:190–201
- [26] Ermakova MA, Ermakov DY, Kuvshinov GG, Plasova LM (1999) New nickel catalysts for the formation of filamentous carbon in the reaction of methane decomposition. *J Catal* 187:77–84
- [27] Ermakova MA, Ermakov DY, Kuvshinov GG (2000) Effective catalysts for direct cracking of methane to produce

- hydrogen and filamentous carbon part I. Nickel catalysts. *Appl Catal A* 201:61–70
- [28] Chinthaginjala JK, Seshan K, Lefferts L (2007) Preparation and application of carbon-nanofiber based microstructured materials as catalyst supports. *Ind Eng Chem Res* 46(12):3968–3978
- [29] Wang H, Terry R, Baker K (2004) Decomposition of methane over a Ni-Cu-MgO catalyst to produce hydrogen and carbon nanofibers. *J Phys Chem B* 108:20273–20277
- [30] Takenaka S, Kobayashi S, Ogihara H, Otsuka K (2003) Ni/SiO₂ catalyst effective for methane decomposition into hydrogen and carbon nanofiber. *J Catal* 217:79–87
- [31] Singh C, Shaffer MSP, Windle AH (2003) Production of controlled architectures of aligned carbon nanotubes by an injection chemical vapour deposition method. *Carbon* 41(2):359–368
- [32] Jong KPD, Geus JW (2000) Carbon nanofibers: catalytic synthesis and applications. *Cat Rev Sci Eng* 42:481–510
- [33] Zhang W, Ge Q, Xu H (2011) Influences of reaction conditions on methane decomposition over non-supported Ni catalyst. *J Nat Gas Chem* 20:339–344
- [34] Zhang W, Ge Q, Xu H (2010) Influences of precipitate rinsing solvents on Ni catalyst for methane decomposition to CO_x-free hydrogen. *J Phys Chem A* 114:3818–3823
- [35] Vieira R, Ledoux MJ, Pham-Huu C (2004) Synthesis and characterization of carbon nanofibers with macroscopic shaping formed by catalytic decomposition of C₂H₂/H₂ over nickel catalyst. *Appl Catal A* 274:1–8
- [36] Ci L, Wei J, Wei B, Liang J, Xu C, Wu D (2001) Carbon nanofibers and single-walled carbon nanotubes prepared by the floating catalyst method. *Carbon* 39:329–335
- [37] Yang KL, Yang RT (1986) The accelerating and retarding effects of hydrogen on carbon deposition on metal surfaces. *Carbon* 24:687–693
- [38] Kim MS, Rodriguez NM, Baker RTK (1991) The interaction of hydrocarbons with copper-nickel and nickel in the formation of carbon filaments. *J Catal* 131:60–73
- [39] Zavarukhin SG, Kuvshinov GG (2004) The kinetic model of formation of nanofibrous carbon from CH₄-H₂ mixture over a high-loaded nickel catalyst with consideration for the catalyst deactivation. *Appl Catal A* 272:219–227